Faraday Discussions

Accepted Manuscript

This manuscript will be presented and discussed at a forthcoming Faraday Discussion meeting. All delegates can contribute to the discussion which will be included in the final volume.

Register now to attend! Full details of all upcoming meetings: http://rsc.li/fd-upcoming-meetings

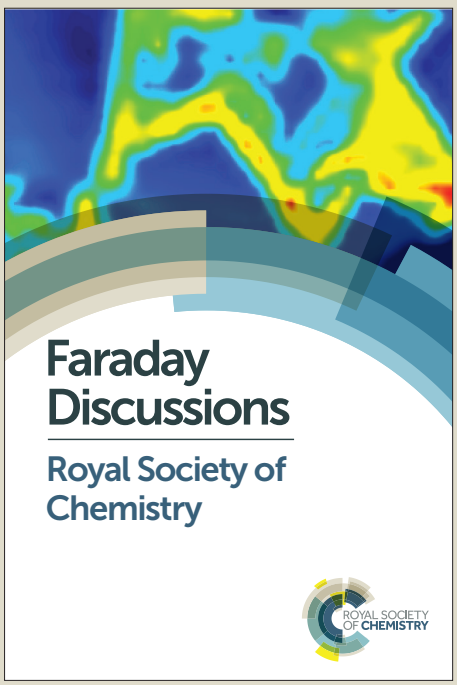

This is an *Accepted Manuscript*, which has been through the Royal Society of Chemistry peer review process and has been accepted for publication.

Accepted Manuscripts are published online shortly after acceptance, before technical editing, formatting and proof reading. Using this free service, authors can make their results available to the community, in citable form, before we publish the edited article. We will replace this *Accepted Manuscript* with the edited and formatted *Advance Article* as soon as it is available.

You can find more information about *Accepted Manuscripts* in the Information for Authors.

Please note that technical editing may introduce minor changes to the text and/or graphics, which may alter content. The journal's standard Terms & Conditions and the Ethical guidelines still apply. In no event shall the Royal Society of Chemistry be held responsible for any errors or omissions in this *Accepted Manuscript* or any consequences arising from the use of any information it contains.

ROYAL SOCIETY OF CHEMISTRY

www.rsc.org/faraday_d

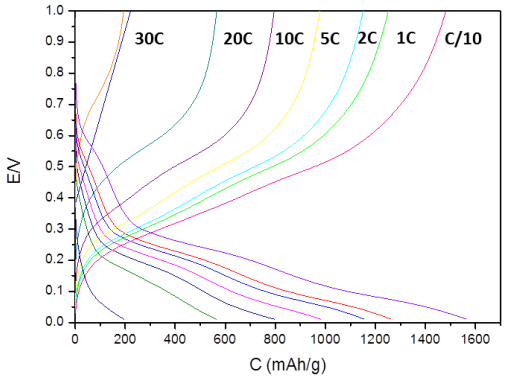

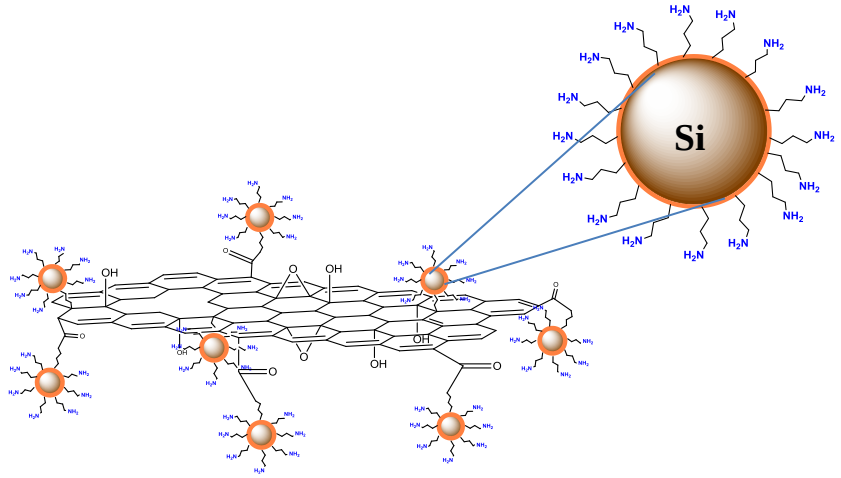

Do we Need Covalent Bonding of Si nanoparticles on Graphene Oxide for Li-ion Batteries?

Yana Miroshnikov, Gal Grinbom, Gregory Gershinsky, Gilbert D. Nessim, David Zitoun*

Abstract

In this manuscript, we report our investigation of anode materials for Li-ion batteries based on silicon-graphene oxide composites. Previous reports in the literature on silicon-graphene oxide (GO) composites as anode have shown a large discrepancy between the electrochemical properties, mainly capacity and coulombic efficiency. In our research, the surface chemistry of Si nanoparticles has be functionalized to yield a chemical bond between the Si and GO, a further annealing step yields Si-reduced GO (Si-rGO) composite while controlled experiments have been carried on mechanical mixing of GO and Si. For all samples, including a simple mixing of Si nanoparticles and GO, a high specific capacity of 2000 mAh/g_{Si} can be achieved for 50 cycles. The main difference between the samples can be observed in terms of coulombic efficiency, which will determine the future of these composites in full Li-ion cells. The Si-rGO composite shows a very low capacity fading and a coulombic efficiency above 99%. Furthermore, the Si-rGO composite can be cycled at very high rate until 20 C (charge in 3 minutes).

1. Introduction

Silicon is extensively investigated as anode material for lithium-ion batteries (LIBs), due to its high theoretical capacity (4,200 mAh g^{-1}) and its natural abundance.[1] However, silicon undergoes a large volume change of 300-400% upon cycling, which leads to electrode cracking and failure of the battery at some point. [2] Many strategies to overcome these challenges have been proposed, such as the use of nanoparticles dispersed in a binder, the preparation of composites and the use of amorphous Si.[3–5] Yet, all these strategies have shown their limitations and a practical solution for overcoming the problems associated with silicon anode is far from being found.

Graphene, a one atom thick, sp^2 bonded carbon layer, has been widely studied, due to its properties in terms of conductivity, flexibility and large surface area. Graphene can be produced through many different routes, such as CVD growth, epitaxial growth on SiC and graphene oxide (GO) reduction. [6–9] Reduced GO (rGO) remains flexible, displays chemical reactivity, can be dispersed in solvent and is conductive enough for electrochemical applications. [10–13]

Therefore, the elaboration of Si-rGO composite materials, where Si nanoparticles (NPs) are anchored on the rGO layers, might be a way to ease the effect of the large volume change. A few routes have been already explored to synthesize these nanocomposites using mixing procedures of either rGO or GO with Si NPs.[14–17] Several principles govern the elaboration of composites; Si NPs should be homogeneously spread on GO and the bonding in the composite has to be strong but flexible to accommodate for the volume changes of Si.[18] Research groups reported on composites of GO and Si NPs by mechanical mixing and obtained Si/rGO nanocomposite paper.[19] Others report on the chemical grafting of Si NPs on GO.[20–22] The nanocomposite shows better performance than the pristine Si NPs but the specific capacity rapidly fades after a few tens of cycles which draws a serious concern on the benefits of rGO in composite anodes. Moreover, the significantly large distributions of values found in the literature for the same composite commands a detailed study of the impact of each synthetic step on the electrochemical properties.

In this research, a Si NPs - GO composite is prepared by modification of the surface of Si NPs, covalent bonding to GO and further annealing to yield Si-rGO. The influence of each step is monitored by a full spectroscopic and microscopic characterization of composites. Each composite (before grafting Si/GO, after grafting Si-GO and after annealing Si-rGO) is tested as anode material in Li-ion batteries to understand the significance of each chemical treatment. For all the samples, a high specific capacity has been achieved but significant differences in coulombic efficiency can be attributed to the chemical nature of the Si-GO bonds.

2. Materials and methods

Silicon nanoparticles of sub-50 nm size (nanopowder 98%, Aldrich), 3-Aminopropyltriethoxysilane (APTES) (ACROS, 99%), graphite flakes (ASBURY carbons), Mesitylene (FLUKA≥99%), H_3PO_4 (ERBA 85%), H_2SO_4 (96%, FRUTAROM), $KMnO_4$ (ALDRICH ≥99.0%), H_2O_2 (FISHER >30%) used as received.

Synthesis of Graphene Oxide (GO). GO is obtained by using an improved Hummers method.[23] Briefly a 9:1 mixture of concentrated H_2SO_4/H_3PO_4 (120:13.3 ml) was added to a mixture of graphite flakes (1.0 g) and $KMnO_4$ (6.0 g) producing a slight exotherm to 35-40 °C. The reaction mixture was then heated to 50°C and stirred for 12 hours. The mixture was cooled to room temperature and poured into ice (~133 mL) with 30% H_2O_2 (1.0 mL). The filtrate was centrifuged (4000 rpm for 4 hours) and the supernatant was decanted away. The remaining solid material was then washed in succession with DI water and ethanol. Then the obtained suspension was centrifuged (4000 rpm 30 min), the supernatant was decanted away and the filtrate was vaccum-dried overnight. A purified graphite oxide was dispersed in water and bath sonicated for 30 min to obtain graphene oxide (GO).

Grafting of APTES (aminopropyltriethoxysilane) on silicon nanoparticles surface. 0.3 g of Si nanopowder is dispersed by magnetic stirring in 20 ml of mesitylene degassed under N_2. 0.318 mL of APTES is added dropwise at room temperature and stirred at 170°C under N_2 for 4 hours. The dispersion is centrifuged at 6000 rpm for 10min to precipitate the brown colloids and redispersed in ethanol, the procedure is repeated twice to remove the excess of silane. The sample is then dried under vacuum for 12 hours.

Synthesis of GO and reduced GO (rGO)- Silicon composite. A few drops of HNO_3 (0.078 $mol.L^{-1}$) are added to APTES terminated silicon nanoparticles dispersed in water, and the pH is brought to ~3. GO dispersion in water is added to the silicon dispersion. The dispersion is heated to 80 °C and stirred for 72 hours. The mixture is cooled to room temperature and freeze-dried at -105 °C overnight to yield the **Si-GO** compound. The eventual reduction step is achieved by placing the dry sample in a tubular furnace under forming gas (Ar/H_2 95/5, 99.999%). The sample is heated to 1000°C using a one hour ramp heating procedure and maintaining the temperature for 5 min at 1000°C, to yield reduced GO-Silicon (**Si-rGO**) composite. The as prepared samples are transferred and stored in a glove box filled with argon.

Alternatively, a mixture of pristine Si NPs is used in place of APTES terminated Si NPs following the same procedure with GO (heating in mesitylene under N_2 at 170 °C for 4 hours). The resulting brown nanopowder is named **Si/GO** sample assuming a non-covalent bonding between Si and GO.

Characterization.

The structure of silicon NPs is investigated by transmission electron microscopy (TEM) on a FEI Tecnai-12 operated at 120 kV or a JEOL JEM-1400 (LaB_6) at 120 kV. The sample is prepared by drop-casting a sonicated dispersion in ethanol on a Lacey carbon grid.

Raman spectra of the samples are collected on a Jobin-Yvon Horiba Raman spectrometer equipped with Olympus BX41 microscope (x 100 lens) and the Raman spectrometer uses a red laser source.

FT-IR spectra of the samples are collected on a Thermo Scientific Nicolet IS20 in ATR mode on a diamond window in the 4000-400 cm^{-1} region.

Electrodes of nanocomposites

All the work has been achieved in an Ar filled glovebox. The dry composite powder has been laminated onto a roughened copper foil (Oxygenfree, SE-Cu58, Schlenk Metallfolien GmbH & Co. KG). The powder has been equally spread on the surface and adhesion to the current collector has been enhanced by applying a manual pressure with a Kimwipes paper. For the electrochemical half-cell studies of the composite, we have used an electrode with surface area of 1 cm^2.

Coin cells

Anodes are tested in coin-type cells (2523, NRC, Canada) vs. lithium metal (Chemetall Foote Corporation, USA). Electrolyte solution is a mixture of fluoro-ethylene carbonate (FEC, Aldrich, < 20 ppm water) and dimethyl carbonate (DMC,Aldrich, < 20 ppm water) (1:4 ratio) with 1 $mol.L^{-1}$ $LiPF_6$ (Aldrich). The cells are assembled in an argon-filled glove box, with a purifying system (MBraun GmbH, Germany), oxygen and water contents below 1 ppm.

Coin-cells are cycled at 30°C using BT2000 battery cycler (Arbin Instruments, USA) (three cycles at C/10, therefore C rate: all capacity in 1 hour). The active mass of silicon anodes is measured by dissolving the Si and dosing with ICP-AES three times.

3. Results and discussion

The synthesis of three samples of Si nanoparticles/graphene oxide (Si NPs/GO) composite is achieved following the experimental procedure described in the experimental section. First sample, named Si/GO is obtained by simple mixing of the two nanomaterials, and should not present any covalent bonding between the GO sheets and the Si surface. During the synthesis and centrifugation, this sample clearly shows two different phases, according to their difference in color: the dark upper phase of graphene oxide and a brown lower phase of the Si NPs. Another sample, named Si-GO is synthesized by covalently bonding between GO sheets and Si surface. This sample is prepared by reacting APTES (aminopropyltriethoxysilane) grafted Si nanoparticles with GO sheets under reflux in mesitylene, yielding a nucleophilic attack of the amine group on the epoxy and carboxylic groups of the GO. During the synthesis, this sample forms a single continuous brownish phase. The as-prepared Si-GO sample can be annealed in a reducing atmosphere to produce a black powder of Silicon reduced graphene oxide, a sample named Si-rGO.

APTES, a widely used grafting agent, [24] is chosen for the functionalization of Si surface. This compound yields a propylamine chain, short enough for electron hopping between GO and Si. Moreover, the siloxane group can easily bind to the native oxide surrounding the Si NPs through a sol-gel process, while the amine group can react on the epoxy and carboxyl groups present in GO to yield a covalent bond. Scheme 1 describes the detailed synthesis route for the preparation of covalently bonded Si-GO composite. Only this sample has been annealed to reduce the GO and the SiO_2 shell since the Si/GO composite without covalent bonds does not show a good homogeneity.

Figure 1 presents the TEM images of Si NPs after APTES grafting (A, B), graphene oxide (C) and an AFM image of graphene oxide (D). Si NPs are dispersed on the TEM grid, and tend to agglomerate into large aggregates. Electron diffraction analysis exhibits the typical diffraction of the cubic crystal structure of silicon (Fd-3m, a = 5.4309 Å, JPCDS 27-1402). The GO sheets exhibit a typical wrinkled morphology, with sheets larger than 3 μm (from TEM observation) and average thickness of 1.5 nm (from AFM images). This suggests that the as prepared GO are three layers thick. Figure 2 displays the TEM images of the as prepared composites, Si-GO (A, B, C), Si-rGO (D, E) and Si/GO mix (F). Si-GO sample (A, B) reveals the presence of GO sheets wrapped up on Si nanoparticles and the electron diffraction shows only the cubic crystalline phase of Si nanoparticles; the Si NPs still form agglomerates which are attached to the GO sheets and dispersed on their surface. Dark field TEM (Fig. 2C) reveals crystalline Si spread on amorphous GO sheets. The Si-GO sample slightly differs from the scheme presented on Fig.1 since the GO sheets follow the morphology of Si NPs and wrap up the particles. Si-rGO sample also shows rGO sheets wrapped up on Si (Fig. 2C-D). The morphology of the two samples can hardly be distinguished, allowing us to compare the two samples assuming a simple chemical reduction of the GO and the Si surface, while the overall morphology remains. In Si/GO mixed sample, graphene oxide sheets are not seen on the entire TEM grid and only Si nanoparticles are spread on the TEM grid (Fig. 2F).

Raman spectroscopy of carbon materials is an excellent technique to measure the quality of the carbonaceous material synthesized, it can be used for the characterization of the graphitic carbon (G-band) and disordered carbon (D-band). The G-band corresponds to sp^2 bonds of graphitic carbon, and the D-band is related to defects. Figure 3 summarizes the Raman spectra of the Si-GO and Si-rGO composite, while pristine GO and surface modified Si NPs are displayed as controlled samples.

The peaks at 1330 cm^{-1} and 1590 cm^{-1} correspond to the D band and the G band, respectively, indicating the carbon fingerprint and the defects arising from the harsh oxidation, a typical GO spectrum. However, we can see that Si-GO and Si-rGO also exhibit a peak at 520 cm^{-1}, which corresponds to the presence of crystalline Si in the produced composite. Important to mention, that after thermal annealing of the Si-GO sample, the intensity ratio of $\mathbf{I_D/I_G}$ has increased from 1.29 for Si-GO to 1.39 for Si-rGO, indicating the reduction of GO to rGO.[25–28]

Figure 4 presents the FTIR spectra of APTES treated Si nanoparticles (Si-NH_2), Si and GO without covalent bonding (Si/GO), Si graphene oxide composite (Si-GO) and GO. The large peaks at 1093 cm^{-1} that is present in Si-NH_2, Si-GO and Si/GO samples are assigned to Si-O-Si stretching vibrations, what indicates the SiO_x presence on the surface of the Si nanoparticles. The GO sample spectra displays a peak at 1757 cm^{-1} attributed to carboxylic groups (-COOH). A broad peak at ~1200 cm^{-1} can be attributed to the epoxy species present in the GO and a peak at 1511 cm^{-1} indicates the presence of alcohols. Si-GO sample shows two characteristic peaks at 1550 cm^{-1} and 1690 cm^{-1} for CNH stretch and C=O amide group. These peaks indicate the presence of the covalent bonds formed during the grafting. The FTIR spectrum of Si-rGO shows a significant decrease of the Si-O-Si band which can be attributed to the reduction of the native oxide. Noteworthy, a new band at ~1400 cm^{-1}, consistent with a Si-C bond could explain the passivation of the sample by the formation of a silicon carbide layer, as demonstrated on nanocomposite of SiO_2/C submitted to a reducing atmosphere.[29] The peak at ~1635 cm^{-1} can be attributed to the remaining chemical groups in reduced GO.[30]

All the materials are tested as anode in Li-ion half cells vs Li metal. The electrode is prepared following the procedure reported in the experimental part. In brief, the composite is spread on a roughened Cu foil as a thin film and inserted in a coin cell vs Li metal with an electrolyte solution of $LiPF_6$ 1 mol/L in fluoroethylene carbonate/dimethylcarbonate (FEC/DMC) 1:4 ratio. Cycling is performed at 1C (charge in 1 hour and discharge in 1 hour) and at a controlled temperature of 30°C.

Figure 5 presents the specific capacities measured for Si-GO composite, Si-rGO composite, Si/GO mix and the coulombic efficiency of each sample. All capacities are normalized to the mass of Si since our controlled experiment on pure GO do not show any reversible electrochemical activity of GO in the window of cycling potential (0-0.8V). All composites exhibit high specific capacity above 1400 mAh/g. The composite prepared by mixing demonstrate the best capacity after 50 cycles (almost 2000 mAh/g) but rapidly fades to show poorer performances than the Si-GO covalently bond sample after 300 cycles. The same trend can be

observed with Si-GO compared with Si-rGO. Obviously, the GO stands as a good substrate for the Si and the direct bonding mitigate the capacity fading. The coulombic efficiency of Si-rGO composite allows a quantification of this observed trend. All coulombic efficiencies are higher than 97%. Nevertheless, the coulombic efficiency of Si-rGO rapidly reaches 99% after 50 cycles while Si-GO reaches a slightly lower value after 150 cycles. Si/GO shows a better efficiency for 30 cycles and poorer performances than the other composites after 100 cycles.

Figure 6 presents the specific capacity measured for Si-rGO composites for more than 1000 cycles. As observed previously, the Si-rGO composites demonstrate a very stable specific capacity after the first 3 cycles, the value stabilizes at 1400 mAh/g after 100 cycles until 1000 cycles. The batteries continue their cycle life further without any noticeable capacity fading. The batteries have maintained their capacity for more than 1000 cycles.

The Si-rGO composites have been tested at different speed of charge/discharge cycling. This capacity rate has been performed after 1000 cycles. Figure 7 displays the charge capacities and voltage profile of Si-rGO composite at different rates from C/10 (10 hours) up to 60C (1 min). The composite exhibits a stable capacity at all the given rates. At 20C, full charge and discharge during 3 minutes each, though the capacity has dropped to 600 mAh/g, the composite still outperforms graphite by a factor of two and the anode material demonstrates reversible performance. In a logarithmic scale, the capacity decreases linearly with the rate until 20C. Beyond this rate (60C), the capacity significantly drops to less than 200 mAh/g. Interestingly, when the rate decreases to C/10, full charge and discharge during 10 hours each, the battery capacity is fully restored. The voltage profile of rGO-silicon exhibits the typical characteristics of Si undergoing lithiation and delithiation, showing two plateau of potential. At voltages between 0.7V to 0.3V another peak, which can be attributed to the rGO, is present.

The first significant result from our investigation is the TEM observation of complete segregation of GO and Si on the TEM grid following a simple Si/GO mix even when performed in the same conditions of temperature and solvent as the covalent grafting (Fig. 2F). However, the grafting of amine function on the surface of Si and the further formation of amides on GO yields a composite of nicely dispersed Si NPs on GO substrate.

All the sample studied have shown very good performances as Li-ion anodic materials for 50 cycles, with very high specific capacity compared to the values reported in the literature. From the capacity measurements (Fig. 5), Si-GO exhibits the highest gravimetric capacity, around 2000 $mAhg^{-1}$ after 50 cycles. The best composite reported in the literature reaches an initial discharge capacity of about 1,750 mAh g^{-1} and 1,000 $mAhg^{-1}$ after 200 cycles. [22,21]

Beyond this number of cycling, the Si-GO is getting closer to the Si/GO without covalent bonding showing a capacity fading This higher value obtained for the Si-GO composite might be attributed to the fact that Si nanoparticles are evenly distributed on GO which even wrap up the Si NPs. The Si NPs are enclosed in the GO, as shown on the TEM images on Fig.2 A-C, while a simple mixing does not provide a nanoscale mixing of Si NPs and GO. The spectroscopic evidences (Raman and FTIR) for the formation of a composite underlines the formation of an amide bond between the amine grafted particles and the reactive species of GO (epoxy and carboxylic groups). This amide bond is strong enough to graft the Si NPs on top of GO, or reciprocally GO on top of Si NPs. Nevertheless, this amide bond is also sensitive to the chemical potential. While the anode is cycled between 0 and 1.0 V versus Li, amide may react at such a negative potential (-3.0 to -2.0 V vs ENH). One interpretation of the capacity fading could be the reactivity of the amide bond upon cycling, partially releasing the Si from its GO substrate. This bond breaking would explain the behavior of Si-GO which resembles Si/GO after 100 cycles in terms of specific capacity and coulombic efficiency.

Therefore, covalent bonding appears to be an essential synthetic step to graft the electrochemically active Si on its GO substrate. While this step provides an effective composite until 50 cycles, stronger chemical bonds are needed to endure the harsh conditions of potential in the battery.

Therefore, we use the covalent grafting followed by an annealing step to yield Si-rGO composites. As shown by TEM on Fig. 2D-E, the Si NPs are now completely wrapped up by the carbonaceous material which provides a robust matrix. After the annealing of Si-GO composite in reducing atmosphere, the aromatic network of GO is partially restored and the defects density is diminished (ref), as evidenced by Raman spectroscopy (Fig. 3). The annealing step therefore benefits to the 2D order of GO (now rGO) and should improve its electronical properties as reported for similar annealing treatments.[31]

Si-rGO composites retain their capacity as shown from the high values of coulombic efficiency reported on Fig.5 (>99%). Si particles are scattered on the flexible, partially conductive rGO matrix with large amount of void spaces, which prevents the cracking of the electrode after the volume expansion of Si during lithiation. Moreover, the concentration of Si nanoparticles on each sheet is quite high (Fig. 2D-E), which might also produce higher conductivity and prevent contact loss.

Si-rGO composite shows very stable and reversible performance for more than 1200 cycles at C rate (Fig. 6). The composite also shows stable and reversible capacities at different C rates (Fig. 7) and its capacity is fully restored at C/10 rate. In a logarithmic scale, the capacity decreases linearly with the rate until 20C. At this rate which corresponds to a charge of 3 minutes, the weight capacity per silicon is till twice the one of graphite, which is the standard anode used in commercial Li-ion batteries. Moreover, the coulombic efficiency remains stable and higher than 99% during the rate capability measurements.

4. Conclusions

In this work, we demonstrate the synthesis of a composite of Graphene Oxide (GO) and Si Nanoparticles (NPs) as anodic material for Li-ion batteries. The synthetic pathway makes used of the chemical functions of GO and the amine grafted on Si NPs by a sol-gel process to yield a covalently bond Si-GO. In the absence of this treatment, the two materials show segregation on the microscale. The Si-GO composite shows high specific capacities of 2000 mAh/g after 50 cycles compared to 1600 mA/g for the mixed sample. The better capacity is attributed to the homogeneous distribution of Si NPS on GO. A further annealing step is needed to improve the capacity beyond 50 cycles. The Si-rGO composite shows state-of-the-art capacity of 1200 mAh/g after 1000 cycles with a very low capacity fading and a coulombic efficiency above 99%. Furthermore, the Si-rGO composite can be cycled at very high rate and shows high specific capacity even at 20 C (charge in 3 minutes).

Acknowledgments

The authors thank Luba Burlaka for her assistance with TEM and Dr Andras Paszternak for the AFM measurements. This work was supported by the I-CORE program of the planning and budgeting committee and the Israel Science Foundation (2797/11).

Bibliography

1. D. Larcher, S. Beattie, M. Morcrette, K. Edström, J.-C. Jumas, and J.-M. Tarascon, *J. Mater. Chem.*, 2007, **17**, 3759.

2. M.-S. Zheng, Q.-F. Dong, H.-Q. Cai, M.-G. Jin, Z.-G. Lin, and S.-G. Sun, *J. Electrochem. Soc.* , 2005, **152** , A2207–A2210.

3. H. Wu, G. Yu, L. Pan, N. Liu, M. T. McDowell, Z. Bao, and Y. Cui, *Nat. Commun.*, 2013, **4**, 1943.

4. J. Luo, X. Zhao, J. Wu, H. D. Jang, H. H. Kung, and J. Huang, *J. Phys. Chem. Lett.*, 2012, **3**, 1824–1829.

5. E. Markevich, K. Fridman, R. Sharabi, R. Elazari, G. Salitra, H. E. Gottlieb, G. Gershinsky, a. Garsuch, G. Semrau, M. a. Schmidt, and D. Aurbach, *J. Electrochem. Soc.*, 2013, **160**, A1824–A1833.

6. S. Mao, H. Pu, and J. Chen, *RSC Adv.*, 2012, **2**, 2643.

7. D. C. Marcano, D. V Kosynkin, J. M. Berlin, A. Sinitskii, Z. Sun, A. Slesarev, L. B. Alemany, W. Lu, and J. M. Tour, *ACS Nano*, 2010, **4**, 4806–14.

8. Y. Zhu, S. Murali, W. Cai, X. Li, J. W. Suk, J. R. Potts, and R. S. Ruoff, *Adv. Mater.*, 2010, **22**, 3906–24.

9. D. R. Dreyer, S. Park, C. W. Bielawski, and R. S. Ruoff, *Chem. Soc. Rev.*, 2010, **39**, 228–40.

10. B. Wang, X. Li, X. Zhang, B. Luo, M. Jin, M. Liang, S. a Dayeh, S. T. Picraux, and L. Zhi, *ACS Nano*, 2013, **7**, 1437–45.

11. T. Kuila, A. K. Mishra, P. Khanra, N. H. Kim, and J. H. Lee, *Nanoscale*, 2013, **5**, 52–71.

12. C. Fu, G. Zhao, H. Zhang, and S. Li, 2013, **8**, 6269–6280.

13. D. Pan, S. Wang, B. Zhao, M. Wu, H. Zhang, Y. Wang, and Z. Jiao, *Chem. Mater.*, 2009, **21**, 3136–3142.

14. K. Eom, T. Joshi, A. Bordes, I. Do, and T. F. Fuller, *J. Power Sources*, 2014, **249**, 118–124.

15. H.-C. Tao, L.-Z. Fan, Y. Mei, and X. Qu, *Electrochem. commun.*, 2011, **13**, 1332–1335.

16. X. Zhou, A.-M. Cao, L.-J. Wan, and Y.-G. Guo, *Nano Res.*, 2012, **5**, 845–853.

17. R. C. Guzman, J. Yang, M. M.-C. Cheng, S. O. Salley, and K. Y. Simon Ng, *J. Mater. Sci.*, 2013, **48**, 4823–4833.

18. H. Xiang, K. Zhang, G. Ji, J. Y. Lee, C. Zou, X. Chen, and J. Wu, *Carbon N. Y.*, 2011, **49**, 1787–1796.

19. J. K. Lee, K. B. Smith, C. M. Hayner, and H. H. Kung, *Chem. Commun. (Camb).*, 2010, **46**, 2025–7.

20. M. Zhou, F. Pu, Z. Wang, T. Cai, H. Chen, H. Zhang, and S. Guan, *Phys. Chem. Chem. Phys.*, 2013, **15**, 11394–401.

21. G. Zhao, L. Zhang, Y. Meng, N. Zhang, and K. Sun, *J. Power Sources*, 2013, **240**, 212–218.

22. Y.-S. Ye, X.-L. Xie, J. Rick, F.-C. Chang, and B.-J. Hwang, *J. Power Sources*, 2014, **247**, 991–998.

23. D. C. Marcano, D. V Kosynkin, J. M. Berlin, A. Sinitskii, Z. Sun, A. Slesarev, L. B. Alemany, W. Lu, and J. M. Tour, *ACS Nano*, 2010, **4**, 4806–14.

24. A. Simon, T. Cohen-Bouhacina, M. C. Porté, J. P. Aimé, and C. Baquey, *J. Colloid Interface Sci.*, 2002, **251**, 278–83.

25. K. N. Kudin, B. Ozbas, H. C. Schniepp, R. K. Prud'homme, I. a Aksay, and R. Car, *Nano Lett.*, 2008, **8**, 36–41.

26. X. Díez-Betriu, S. Álvarez-García, C. Botas, P. Álvarez, J. Sánchez-Marcos, C. Prieto, R. Menéndez, and A. de Andrés, *J. Mater. Chem. C*, 2013, **1**, 6905.

27. A. C. Ferrari and D. M. Basko, *Nat. Nanotechnol.*, 2013, **8**, 235–46.

28. S. Piscanec, a. C. Ferrari, M. Cantoro, S. Hofmann, J. a. Zapien, Y. Lifshitz, S. T. Lee, and J. Robertson, *Mater. Sci. Eng. C*, 2003, **23**, 931–934.

29. P.-C. Gao, Y. Lei, A. F. Cardozo Pérez, K. Rajoua, D. Zitoun, and F. Favier, *J. Mater. Chem.*, 2011.

30. H. Zhang, D. Hines, and D. L. Akins, *Dalton Trans.*, 2014, **43**, 2670–5.

31. H. F. Xiang, Z. D. Li, K. Xie, J. Z. Jiang, J. J. Chen, P. C. Lian, J. S. Wu, Y. Yu, and H. H. Wang, *RSC Adv.*, 2012, **2**, 6792.

Scheme 1: The detailed synthesis for the preparation of Si-GO anode composite.

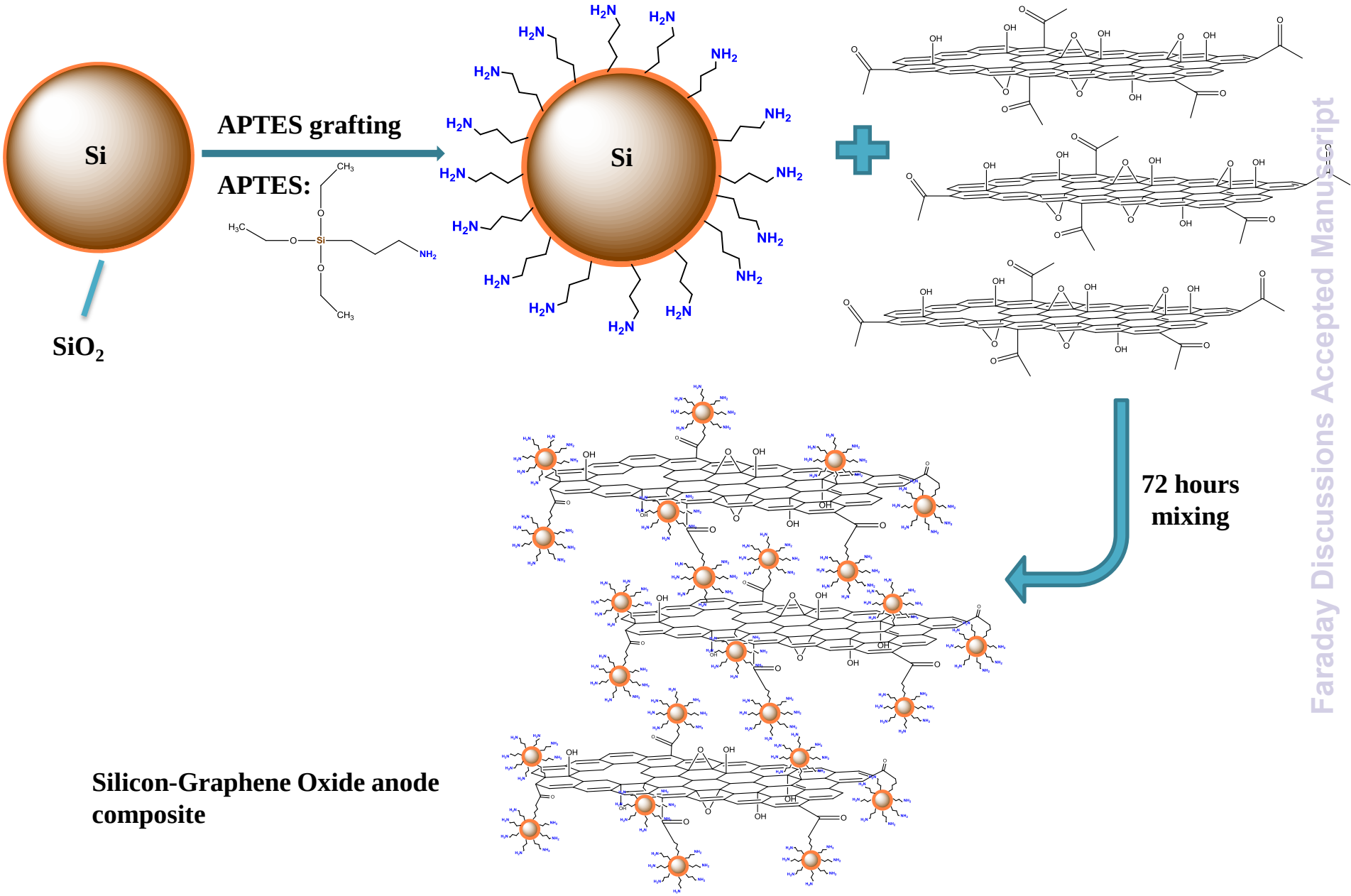

Figure 1: TEM images of Si after APTES grafting (A,B) , graphene oxide (C); AFM image of graphene oxide (D).

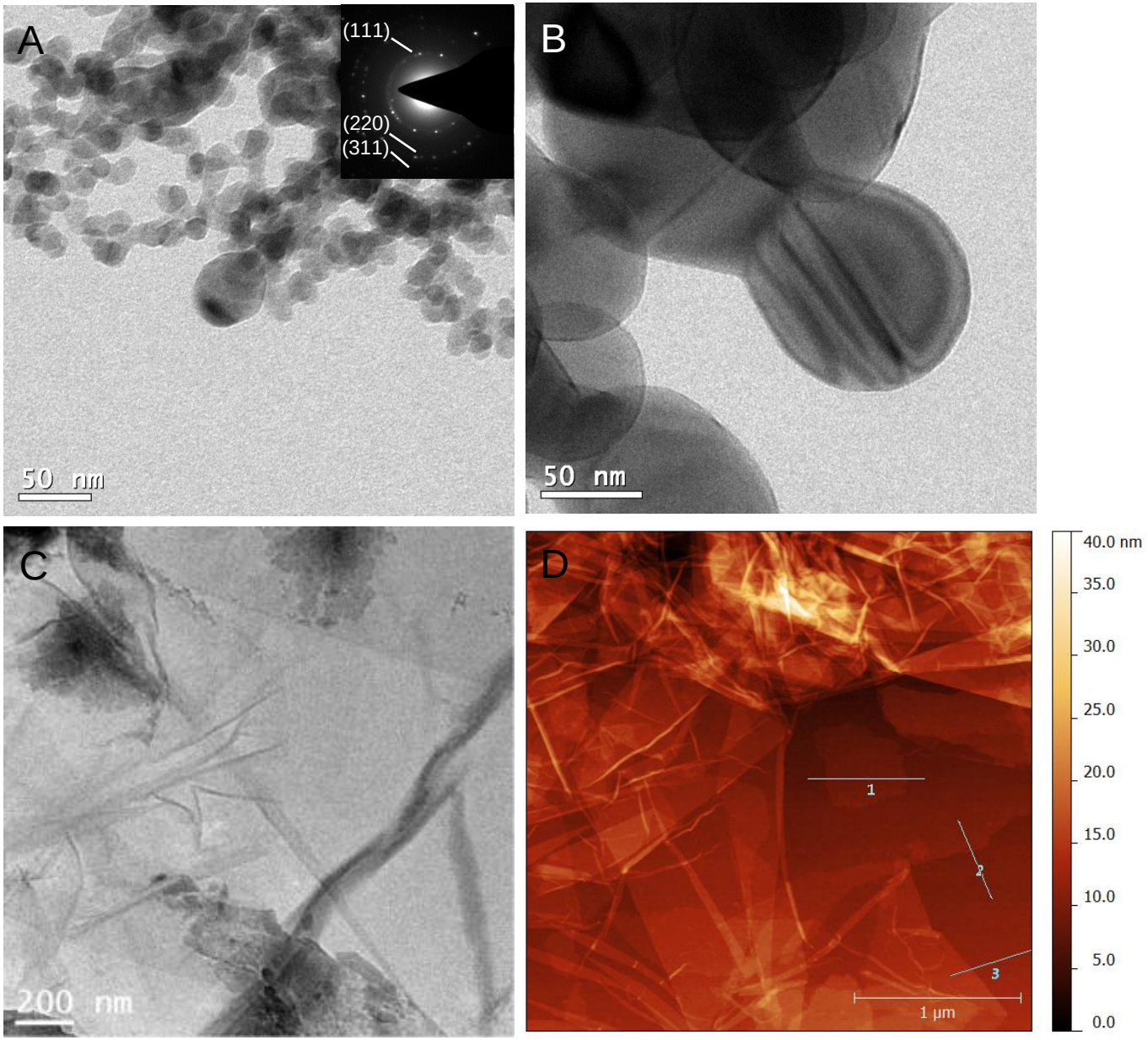

Figure 2 : TEM images of Si-GO composite (A,B,), dark field (C) ,Si-rGO composite (D,E), Si/GO mix (F).

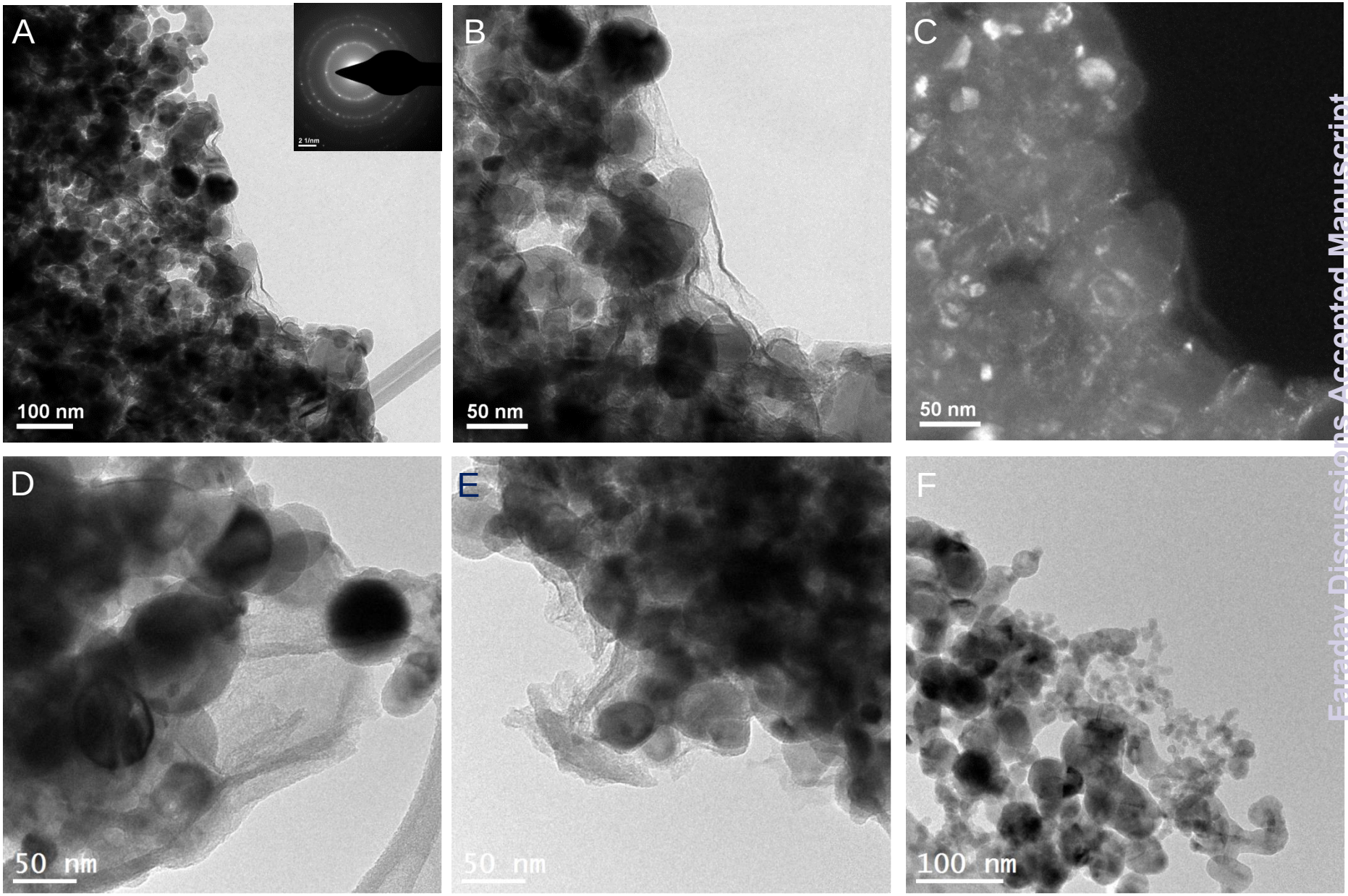

Figure 3: Raman spectra of Si treated with APTES (Si-NH_2), graphene oxide (GO), silicon-graphene oxide composite (Si-GO) and silicon – reduced graphene oxide composite (Si-rGO).

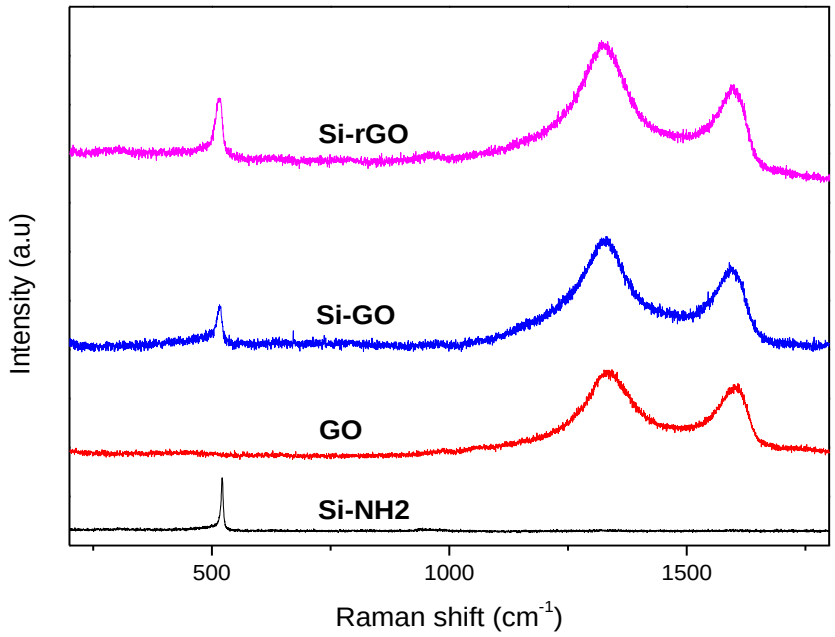

Figure 4: FTIR spectra of graphene oxide (GO), silicon –graphene oxide composite (Si-GO), Si mixed with GO (Si/GO), Si treated with APTES (Si –NH_2)

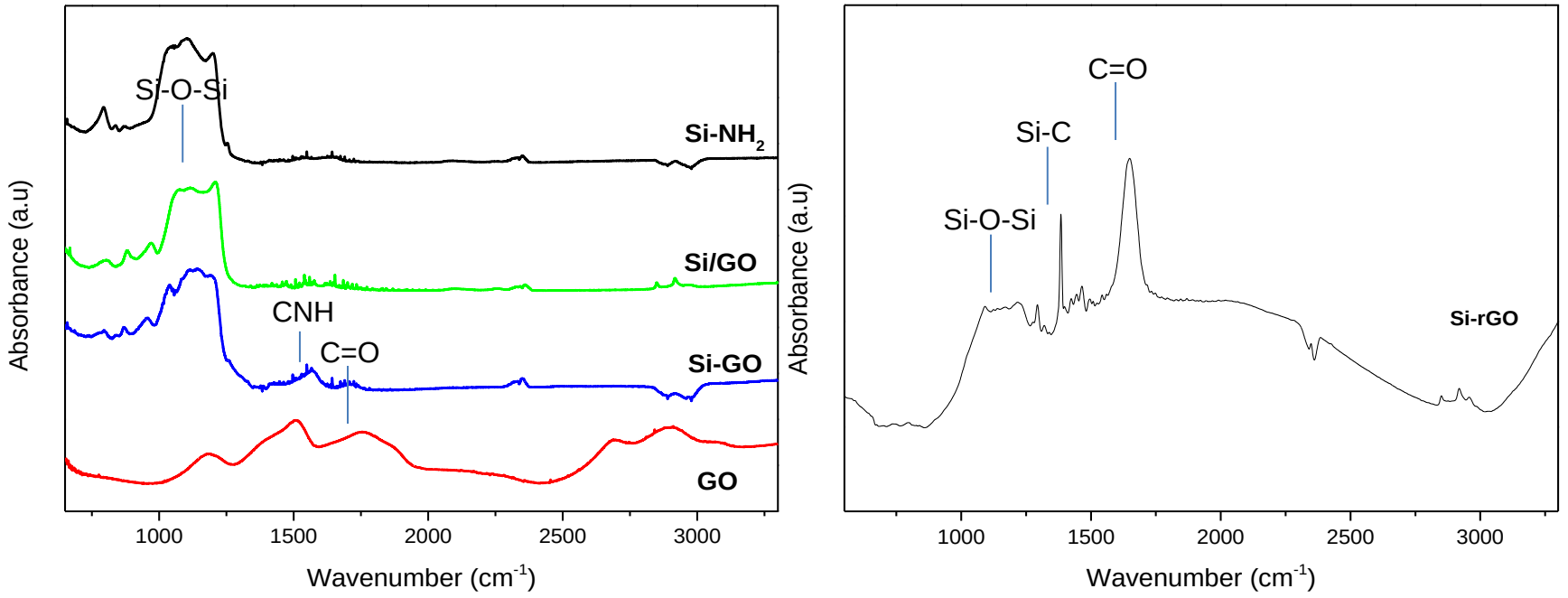

Figure 5 : Cycling performance of Si-GO and Si-rGO composites, compared to Si/GO mix (a); Colombic efficiency of Si-GO, Si-rGO and Si/GO (b).

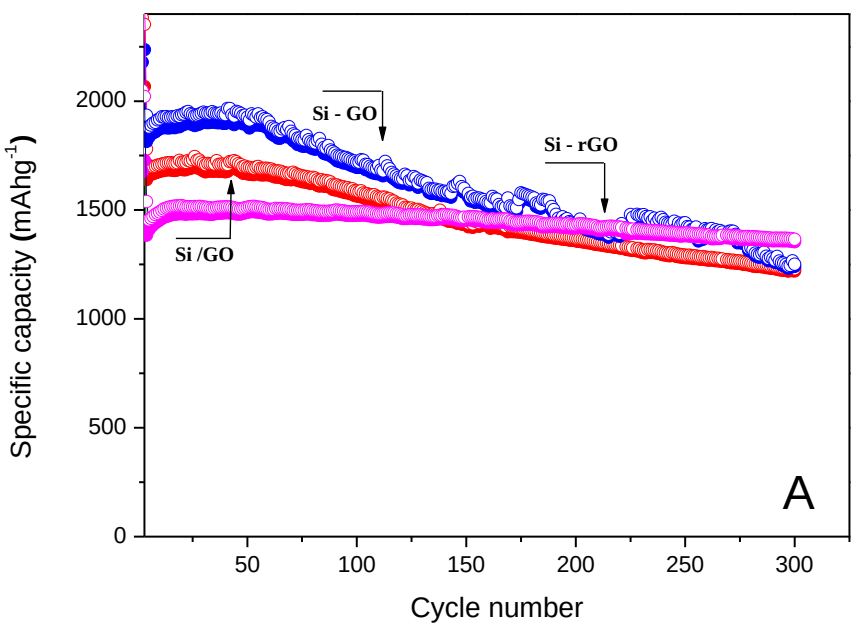

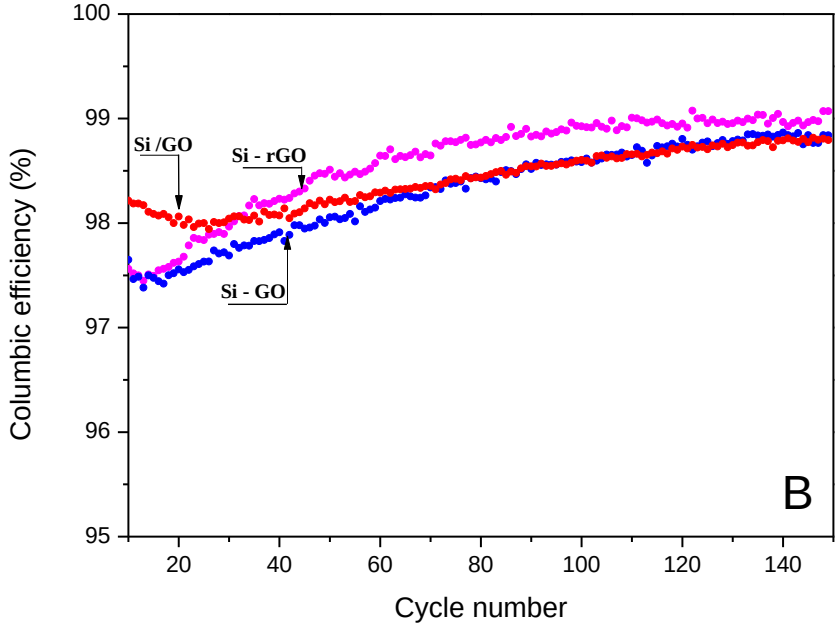

Figure 6: Gravimetric capacity of rGO-Si composite at C rate.

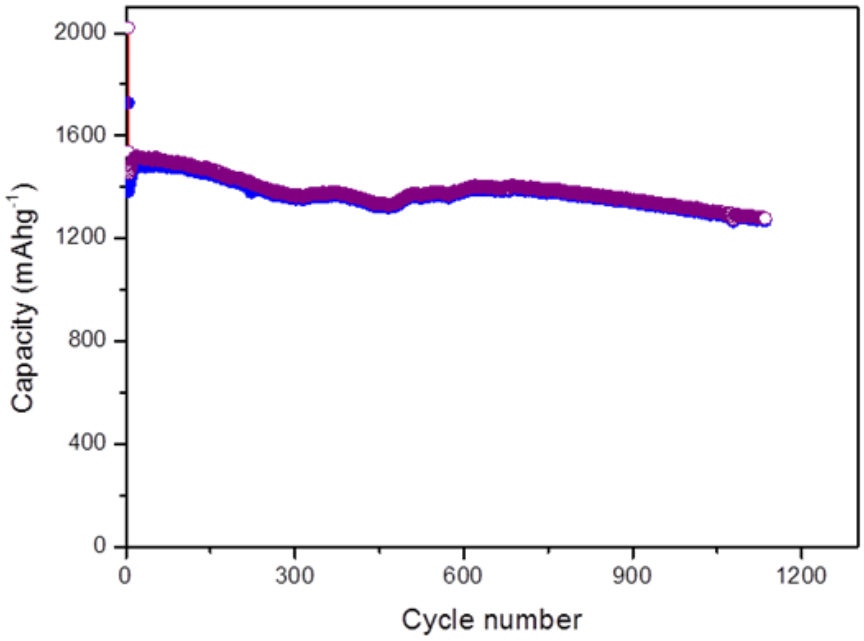

Figure 7: Rate capability of Si-rGO composite (a) at different rates: C/10, C, 2C, 5C, 10C, 20C, 60C; Voltage profile of the composite (b)